

Energy 395 - Bass Connections in Energy: Innovation and Design

Photovoltaic-Thermal Solar Energy System

Woodley Burrow, Katie Cobb, Powell Lowe, Kevin Peng, Will Rawlings,

Ashley Rosen, Swetha Sekhar

Professors: Drs. Emily Klein, Josiah Knight, and Eric Rohlving

Table of Contents

Executive Summary	2
Introduction	3
Background	5
Existing PV Heat Management Techniques	5
Existing Methods to Connect Heat Pipes to Panel	5
Specs of Ordered Heat Pipes	6
Heat Transfer Theory and Initial Calculations	7
Experimentation and Prototype Development	10
Panel Testing	10
Heat Pipe Effective Length	11
Heat Pipe Arrangements	14
Number of Heat Pipes	15
Heat Pipe Angle	16
Flow Rates	17
Panel Backing	20
Final Design	21
CAD Simulations	22
Environmental Benefit Analysis	25
Target Market and Basic Business Plan	27
Other Considerations	31
Conclusion	32
References	33
Appendices	35
Appendix A: Table of System Thermal Properties, Relevant Areas, and Relevant Lengths (Engineering ToolBox. (n.d.))	35
Appendix B: Bill of Materials for Final Prototype	35
Appendix C: Thermal Resistor Network Model	36
Appendix D: Carbon Emission Calculations	36

Executive Summary

As the US transitions away from fossil fuels such as coal and natural gas, alternative energy sources, especially solar power, are expected to become much more important. Currently, solar panels tend to function at around 30% electrical efficiency due to constraints caused by the design of solar panels and excess heat on and in the panel, which slows down electrical interactions (Shockley & Queisser, 1961). The energy that does not become electrical energy becomes heat energy. The goal of this project is to integrate a heat transfer system with a solar panel so that the heat energy from the solar panel can be harnessed for an alternate application, such as heating water, therefore reducing the demand for energy while also increasing the efficiency of the panel by drawing away excess heat. The team's approach was to integrate heat pipes onto a given solar panel, where the evaporator end was aligned with the underside of the solar panel, and the condenser end was inserted into a PVC pipe so that the heat from the panel could be transferred to a working fluid, such as water or air, in the PVC pipe. After experimenting with the heat pipes themselves and the solar panel, an integrated design was built and tested in laboratory conditions to evaluate the feasibility of such a photovoltaic-thermal energy system. While relevant data was collected, the subsequent analysis yielded inconclusive results and showed that the proposed design transferred an insufficient amount of heat to be economically viable. This technology would be feasible in areas of high insolation, interest, and where requirements drive a need for photovoltaic-thermal systems.

Introduction

Photovoltaic (PV) solar power is expected to play a pivotal role in transitioning the world away from reliance on carbon-emitting fossil fuels. This energy transition has already begun in the United States; according to the Energy Information Administration (EIA), the United States added approximately 15.5 gigawatts of solar power capacity to the electricity grid in 2021 (U.S. Energy Information Agency, 2022). To achieve global climate goals, such as net-zero emissions, PV solar power installations will steadily continue in the following decades. The International Energy Agency (IEA) “Net Zero by 2050” report claims that, in a net-zero emissions scenario, renewable sources will make up 88% of global electricity generation, whereas in 2020, renewables only accounted for 29% of generation (International Energy Agency, 2021). PV solar power will positively impact the environment, because, as solar power plants replace coal and natural gas plants, carbon emissions will decrease.

However, PV solar power has several hurdles to overcome in order to occupy a larger share of the energy mix. The team sought to address two of those hurdles in this project. First, solar PV panels with only one p-n junction are limited in how much energy they can produce by the Shockley-Queisser limit, which is based on the fact that only photons of a certain wavelength corresponding to the material’s band gap will be able to create an electron-hole pair. Photons with less energy than the band gap will either pass through the panel or be converted into heat energy on the panel, while photons with more energy will create an electron-hole pair, and the excess energy will also be converted to heat. This means that only a fraction of the incoming energy (approximately 30% for panels with a band gap of 1.1 eV) can actually be converted to electrical energy; the rest of the energy will be lost to reflection or as waste heat (Shockley & Queisser, 1961). Thus, when only electrical energy is harvested from a PV panel, the efficiency

of the panel has an ultimate limit of the fraction of incoming photons within the band gap. Second, solar panels experience a loss in efficiency of, on average, 0.45% per degree above 25 °C (Skoplaki & Palyvos, 2009). Reduced efficiency due to heat is problematic, because solar panels can get very hot as they absorb incoming insolation; under standard conditions, solar panels have been found to reach temperatures well into the 40-50°C range (Ross and Smokler, 1986).

In order to augment a sustainable future that relies on PV solar power, our team designed a PV-thermal system that attempts to capture waste heat and maximize PV solar cell performance. The thermal system is an array of heat pipes attached to the backside of the solar cell. The objective of the project is to test the viability of this PV-thermal system based on heat pipes. A successful design should capture and transfer heat for a secondary use.

Additionally, a successful design should be reproducible and affordable so that the design can be implemented at scale to meet the needs of growing the solar power industry. In capturing waste heat, the team sought to increase the efficiency of the solar panel by utilizing a larger portion of the incoming energy while cooling the panel to maintain optimal operating temperatures. Furthermore, the captured waste heat could be used to preheat a fluid (e.g. water or air), potentially offsetting some of the carbon dioxide emissions produced by traditional heating methods (e.g. natural gas).

Background

Existing PV Heat Management Techniques

Many studies have investigated potential technologies to manage solar panel temperature. There are two classifications for cooling techniques: passive cooling and active cooling. Passive cooling involves processes that do not require additional energy input to cool, while active cooling involves processes that use additional energy to run. Active cooling systems typically see greater reductions in panel temperatures when compared to passive cooling systems (Dwivedi et al., 2020). However, active cooling systems generally have a higher associated cost, especially when extensive fluid piping is required. Heat pipes have been used for both passive and active cooling processes, as they can efficiently transfer heat to a passive cooling system, like a heat fin, or an active cooling system, like a stream of running water (Dwivedi et al., 2020). As one objective of the project was to utilize heat generated by the panel for a secondary process, the team opted to use heat pipes to design for an active cooling system such that the captured heat energy could be transferred via a moving fluid to its secondary purpose.

Existing Methods to Connect Heat Pipes to Panel

In conducting a literature review, the team researched methods used to attach the heat pipes to the solar panel.

Habeeb et al. used a thin copper plate to connect the heat pipes to the panel vertically, where the condenser end of the heat pipe extended past the edge of the panel so that it could be encased in a box on the top edge of the panel, where water was flowing through, so that the excess heat from the panel could heat the water. Habeeb et al. found that this method reduced panel temperature by 15-35%, resulting in a panel efficiency improved by 11-14% when compared to a standard solar panel (Habeeb et al., 2018).

Tonui et al. developed an air-cooled system for PV cells. One configuration they used was to attach heat fins to the back wall of an air duct behind the solar panel. They acknowledged that attaching the fins to the panel directly would better cool the panel but that it was unfeasible for their particular study. The benefit of attaching the heat sink directly to the panel was a key takeaway for the team (Tonui & Tripanagnostopoulos, 2007).

Additionally, Anderson et al. developed a natural convection cooling system with heat pipes for a concentrated solar photovoltaic system. For this study, researchers used an aluminum saddle to attach a heat pipe to the back of a model solar cell, where heat was conducted through the saddle to the heat pipe. They added aluminum fins along the heat pipe to further improve cooling. Unlike Habeeb et. al's study, researchers positioned the heat pipe horizontally (Anderson et al., n.d.).

Ali et al. placed heat pipes vertically along the back of a panel. The back of the panel was insulated and filled with water to transfer heat to the heat pipes. The condenser end of the heat pipes was then submerged in a second system with a water chiller. The researchers found that the cooling system led to an increase in power output of 8% (Ali et al., 2021).

In Zhou et al.'s review of PVT systems with heat pipes, the majority of the systems reviewed had a setup similar to Ali et al. with the heat pipes in the vertical position (Zhou et al., 2021). This motivated the team's decision to place their pipes in the vertical position (see Fig. 7).

Specs of Ordered Heat Pipes

For the thermal system, the team purchased round heat pipes from ATS (Advanced Thermal Solutions) Inc. The copper heat pipes have a nominal outer diameter of 7mm, and a nominal length of 500mm. The team chose this smaller size so that the heat pipes could be attached to the solar cell and so that the heat pipes could be tested in a lab setting. Heat pipes are

traditionally used for compact electronics enclosures, aerospace, medical, consumer electronics, and HVAC applications (Advanced Thermal Solutions). The heat pipes' heat transfer capabilities are described in the "Technical Design" section.

Heat Transfer Theory and Initial Calculations

Heat pipes enhance heat transfer through cyclical phase change processes of evaporation and condensation of an internal working fluid. As heat is applied to one part of the heat pipe (evaporator end), the working fluid vaporizes and moves through the central vapor space to the opposite end of the heat pipe. At this end (condenser end), heat is removed, causing the vapor to condense back into liquid form and travel through a wick lining back to the evaporator end where it is vaporized again.

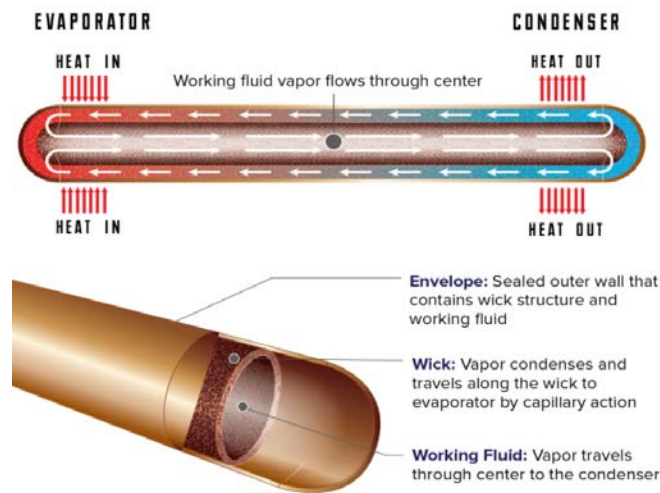


Figure 1. Heat Pipe Function Schematic from Advanced Cooling Technologies (Advanced Cooling Technologies. (n.d.))

The expected heat transfer of the system can be calculated by breaking down the system into a series of 1-D conduction problems at steady state. Heat transfer via conduction is governed by Fourier's Law $q'' = -k \nabla T$, where q'' is the heat flux in W/m^2 , k is the thermal conductivity ($\text{W/m}^2 \cdot \text{K}$), and ∇T is the temperature gradient. This simplifies to

$$q'' = -k \frac{dT}{dx} \quad \text{eq. 1}$$

in 1-D when heat transfer in the y and z directions are much smaller than heat transfer in the x direction. In order to simplify modeling of the system, this approximation is assumed to be true as the thickness in the direction of heat transfer being analyzed is much smaller compared to the thickness in other directions. The heat transfer of the system can be broken down into the following sequential steps:

1. Heat transfer from sunlight to the panel.
2. Heat transfer from panel to heat pipe surface.
3. Heat transfer at the surface of the heat pipe evaporator end radially through the heat pipe wall to the internal heat pipe vapor space.
4. Heat transfer along the length of the heat pipe through the vapor space.
5. Heat transfer from the vapor space radially out to the surface of the condenser end of the heat pipe.
6. Heat transfer from the surface of the heat pipe to cooling fluid.

The first step occurs through radiation rather than conduction. In reality, heat sources are generated within the panel at different depths according to the following formula:

$$\dot{q}_s(x) = -\frac{dI(x)}{dx} = aI_0 e^{-ax} \quad \text{eq. 2}$$

where a is a material property that determines how quickly light is absorbed and I_0 is the initial light intensity. However, since generation of sources would invalidate steady state conditions, the sunlight was modeled as creating a constant heat source applied to the top surface of the panel.

By using the peak solar radiation of Durham, NC (6.46 kWh/m²/day), multiplying by the area of the solar panel from the Gendell Laboratory see *Experimentation and Prototype Development - Panel Testing* for more info), and assuming that all efficiency losses of the panel are converted to heat, the heat applied to the surface of the panel was calculated to be

0.3647-0.5105 of kW/hour/day for 50%-70% conversion of sunlight to heat. Taking the larger value corresponding to a less efficient panel, and assuming steady state conditions for a certain hour in a day, the applied heat is 0.5105 kW.

Given the significant losses present in the experimental model described later, it was decided that mathematical modeling was most useful for a prediction of how much heat is successfully extracted rather than trying to predict how the temperature of the external working fluid is behaving. To do this, eq. 1 is used to build a thermal resistor network, modeling the pathway of the heat through the system as a series of resistive elements. A visual representation is shown in Appendix C. In the experiment, the heat that the panel is exposed to travels through three thermal “resistors”: the panel, the heat pipes, and the moving air. R_1 and R_2 are conductive heat transfer and are modeled according to eq. 4 where L is the length in the direction the heat travel, k is thermal conduction coefficient, and A is the cross sectional area perpendicular to the direction of heat travel. The heat moving from the heat pipes into moving air is a forced convection heat transfer and has thermal resistivity defined by eq. 5, where h is the convective heat transfer coefficient, and A is the heated area exposed to the air.

Using the thermal properties documented in the Appendix A and placing the three resistors in series, a total R of 0.3 is obtained. In line with experimental observation, an estimated ΔT (as shown in Appendix C on the thermal resistor network model of the system) between the heat pipes and the panel of 20 K indicates a power transfer of 61 W using eq. 3. The first takeaway from this model is the importance of reducing the thermal resistance of the system to increase the heat transfer. The second is if a heat transfer of 61 W can be obtained from a panel that is generating 55 W of electrical power, the overall efficiency of the panel will increase substantially.

$$q = \frac{\Delta T}{\Sigma R_t} \quad \text{eq. 3}$$

$$R_{\text{conductive}} = \frac{L}{kA} \quad \text{eq. 4}$$

$$R_{\text{convective}} = \frac{1}{hA} \quad \text{eq. 5}$$

Experimentation and Prototype Development

Panel Testing

Several old solar panels were available in the Gendell Laboratory at Duke University for the team to utilize. The panels used were BP Solar SX 60U solar panels with a warranted P_{max} of 55 W. The panels were tested during January in relatively sunny weather (for winter) at three different angles: 30, 45, and 60 degrees. Voltage and current were measured with a multimeter, and output power was calculated with the formula $P = IV$. The recorded values for each panel are summarized in the table below.

Table 1: Solar Panel Electrical Output Data

Panel	30 degrees			45 degrees			60 degrees		
	Volt	Amp	Watt	Volt	Amp	Watt	Volt	Amp	Watt
1	2.8	2.3	6.44	3.3	2.6	8.58	3.5	3.0	7.00
2	3.0	2.5	7.50	3.4	2.8	9.52	3.6	3.0	10.8
3	2.9	2.3	6.67	3.3	2.7	8.91	3.4	2.8	9.52

After this testing was completed, the team moved on to create a set up inside the Gendell Lab to allow testing during any time of day. It was determined that future experiments would focus on creating the expected heat profile within the panel and not focus on electrical power

output considering the panels' degradation and limited sunlight. To do so, the panel was laid out on an existing wood structure in the lab and then an 80/20 Aluminum structure was used to suspend 3 heat lamps over the panel, as shown below.



Figure 2: Initial Set-Up on Wooden Structure

This set-up was checked to see if temperature was variable across the panel, and it was found that, while it was variable across the panel face, there was little to no variance through the panel. This was similar to what was predicted by preliminary simulations (see “CAD Simulations” section below), so the team then moved on to testing the panel with one heat pipe attached to the underside.

Heat Pipe Effective Length

One important parameter of the heat pipe is its effective length, L_{eff} . The effective length contains information about the relative lengths of the heat pipe that are heated, cooled, and insulated. The portion of the heat pipe that is heated is called the evaporator length, L_e , because the heat applied to this portion of the pipe vaporizes the liquid inside the heat pipe. The length of pipe that is cooled is called the condenser length, L_c , because, as heat is removed from this portion of the pipe, the vapor condenses back into a liquid. The insulated length, L_i , theoretically has no heat transfer, but in reality has a small amount of heat transfer relative to the evaporator and condenser lengths. The effective length can be calculated via the following formula:

$$L_{eff} = L_i + \frac{L_e + L_c}{2} \quad \text{eq. 6}$$

$$k_{eff} = (Q * L_{eff}) / (A * \Delta T) \quad \text{eq. 7}$$

The effective length is inversely related to the heat transferred through the heat pipe. The team conducted multiple experiments to change the amount of insulated length (and therefore the evaporator and condenser lengths) in order to verify these relationships between effective length and temperature difference and heat transferred by the heat pipe.

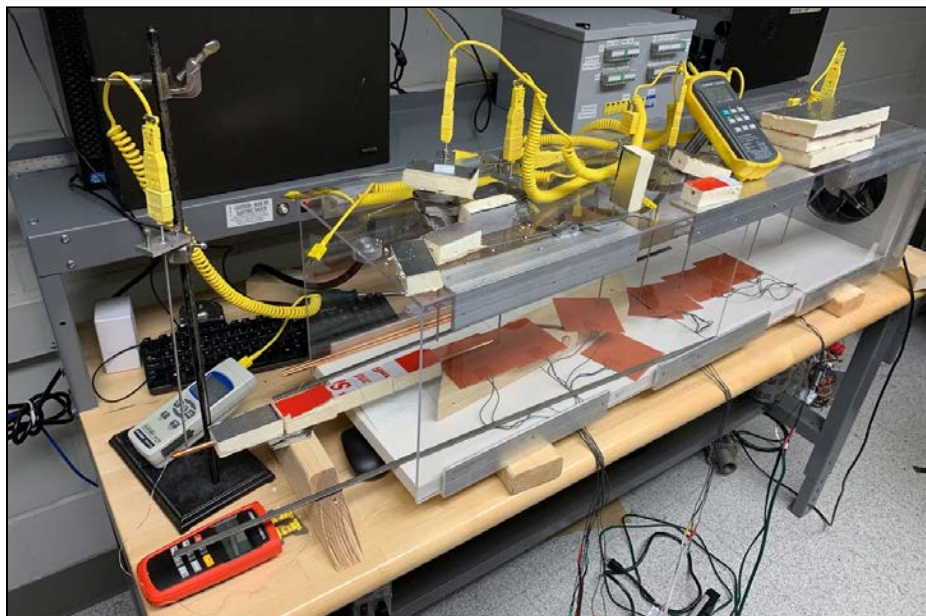


Figure 3. Lab Setup for Heat Pipe Effective Length Experiments



Figure 4. Thermocouples Positioned at Heat Source (Heating Pad) and Heat Sink (Ambient Air Above Condenser Length of Heat Pipe)

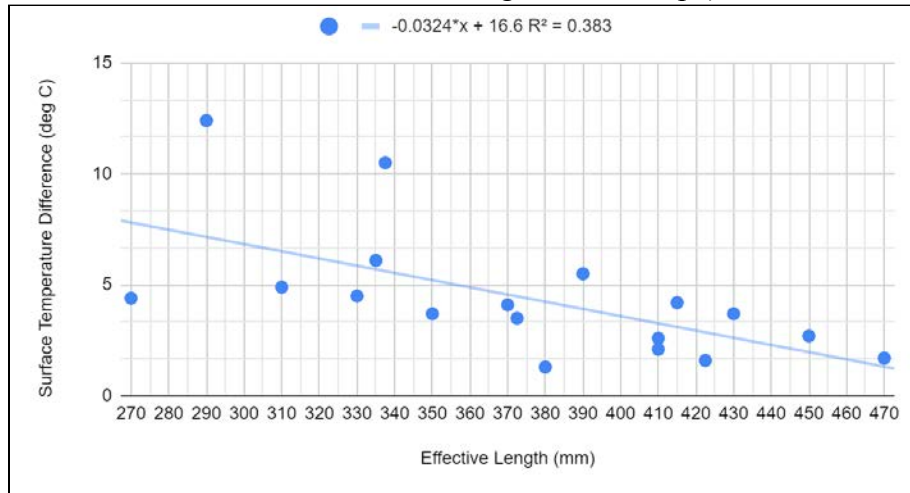


Figure 5. Effect of Effective Length on Heat Pipe Surface Temperature Difference

As the internal vapor temperature difference was not possible to measure without damaging the heat pipe and compromising the device integrity, the surface temperature at each end of the heat pipe was used as an approximate indicator of the heat pipe internal vapor temperature difference. As seen in Figure 5, the data suggests an inverse relationship between the effective length and surface temperature difference, however the data is not statistically conclusive enough to confirm this behavior.

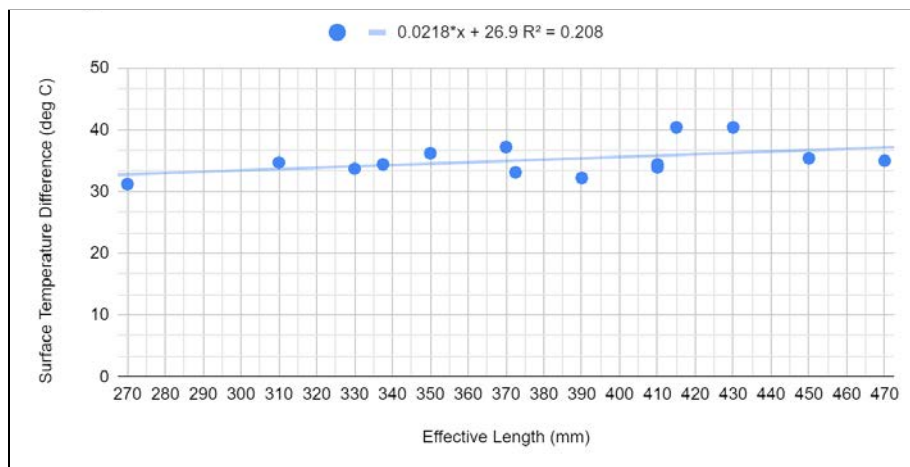


Figure 6. Effect of Heat Pipe Effective Length on Temperature Difference Between Heat Source and Heat Sink

A similar relationship could not be determined for the heat transferred by the heat pipe. The heat transferred by the heat pipe was approximated by measuring the temperature difference between the heat source (a heating pad) and the ambient air around the condenser end of the heat pipe that was cooling this portion of the heat pipe through natural convection. It was speculated that the lack of a noticeable change in heat transfer from the heat source to the sink could be due to lack of sufficient cooling at the condenser end. Therefore, the team moved on to construct experimental setups with cooling via forced air convection at the condenser end.

Heat Pipe Arrangements

Positioning of the heat pipes along the solar panel backing was primarily considered as a design consideration for maximum heat removal and secondarily for cost impacts. In the experiments conducted for this paper, the heat pipes were arranged in a parallel array as shown in Figure 7.

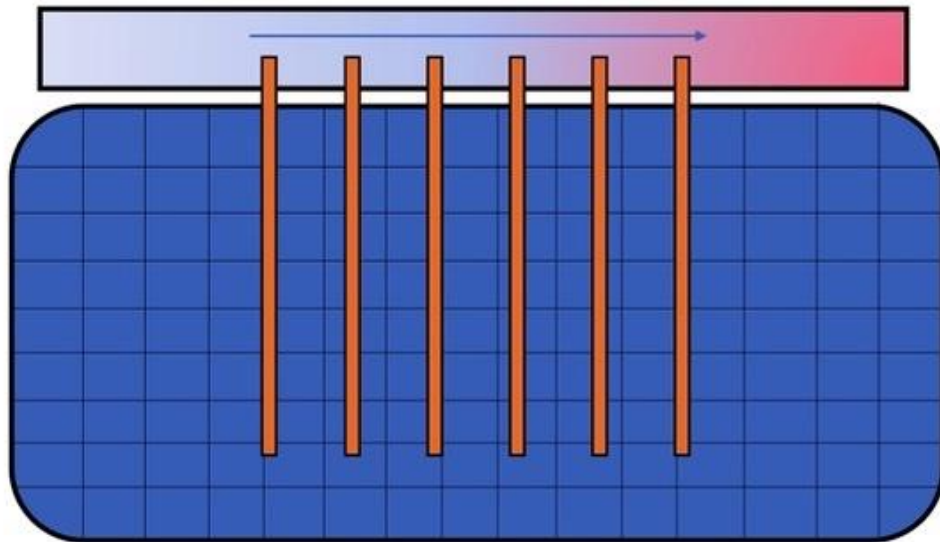


Figure 7: Array of Six Heat Pipes Centered on Back Solar Panel

The hottest section of the panel was located in the middle (since the heat lamps were centered on the panel to get a somewhat even temperature distribution), so the array of heat pipes was centered on the panel and extended towards the edges of the panel backing for as many heat pipes as decided necessary for the given experiment. The configuration presented also allowed for easier installation of the PVC airflow channel on the solar panel's side. Other proposed iterations which should be tested in consequent projects include placing the air channel down the middle of the panel and inserting the heat pipes in the channel from either side as shown in Figure 8. This would allow for the panel to rotate around the air channel and provide potential cost saving when panels are combined with single axis trackers.

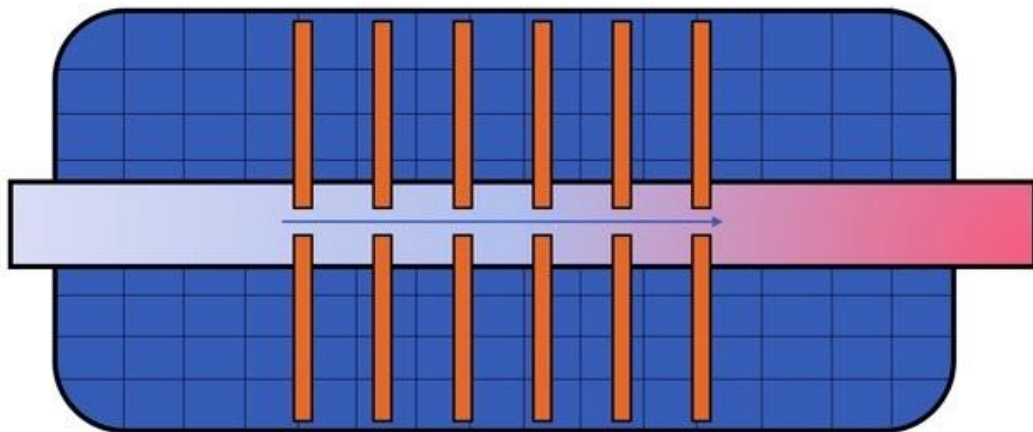


Figure 8: Airflow Channel Repositioned for Single Axis Tracking Panel

Number of Heat Pipes

It was theorized that maximizing the number of heat pipes would be the optimal approach, providing more opportunity for heat to be removed from the panel. Given the challenges of collecting statistically meaningful data of the expressed temperature differences, experiments were not extensively conducted to confirm this theory. However, two trials in which the number of heat pipes was reduced from six to three suggested that the magnitude of the

temperature difference directly correlated to the number of heat pipes in the system. Therefore, there is a larger temperature difference when there is a greater number of heat pipes.

Heat Pipe Angle

The impact of heat pipe orientation has been explored in several studies. The optimal heat pipe orientation depends on several factors, including structure of the heat pipe, working fluid, percentage of space filled with liquid, and power input (Qpedia, 2009). This is because, depending on the wick used for the heat pipe, gravity can either aid or hinder the movement of the fluid within the heat pipe. For copper heat pipes using water as a working fluid and transferring a small amount of heat, it has been found that a 0° orientation angle with respect to the horizontal is the most efficient orientation (Madhuri et al., 2019). To verify this information, a preliminary experiment was conducted by orienting the experimental set up at an approximately 45° orientation angle with respect to the horizontal, as shown in Figure 18. Initial observations did not show a difference in air temperature between the 0° and 45° orientations; thus, the team decided to move forward with the 0° orientation for ease of construction and experimentation.

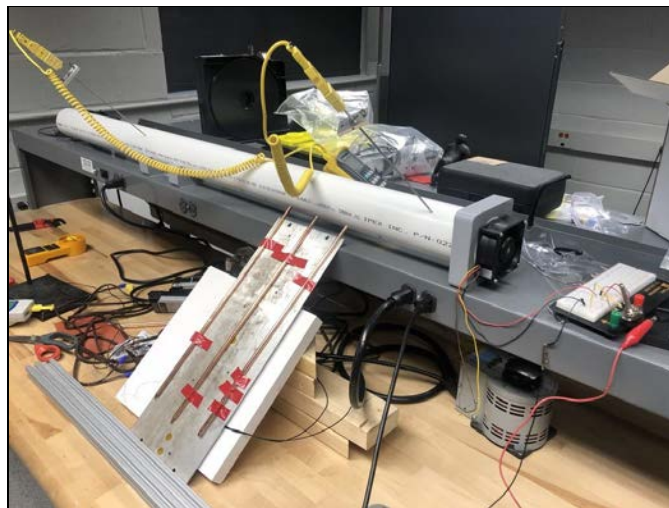


Figure 9: Angled Heat pipe Experimentation Set-Up

Flow Rates

In order to transfer heat out of the system, a flow of working fluid across the ends of the heat pipes needed to be established. To understand how altering the flow rate would impact the change in temperature achieved across the system, an experimental set-up as shown in *Heat Pipe Arrangements*, Figure 7 was used. While air was used as the working fluid for ease of construction, the results found can be extrapolated to using water as the working fluid, should other use cases be desired. The team experimented with varying the speed of the air ranging from approximately 1 to 4 meters per second. The team also experimented with using a flow reducer to further vary the volumetric flow rate. The temperature of the air flow was taken twice, once upstream of the heat pipes and again downstream of the heat pipes, and the temperature difference was calculated. Based on the equation for specific heat capacity, $Q' = m'c\Delta T$, an inversely proportional relationship was anticipated between the flow rate of the air and the temperature of the fluid, assuming that the heat power input by the heat pipes to the moving air was the same. Figure 10 shows the data collected with a reciprocal line of best fit.

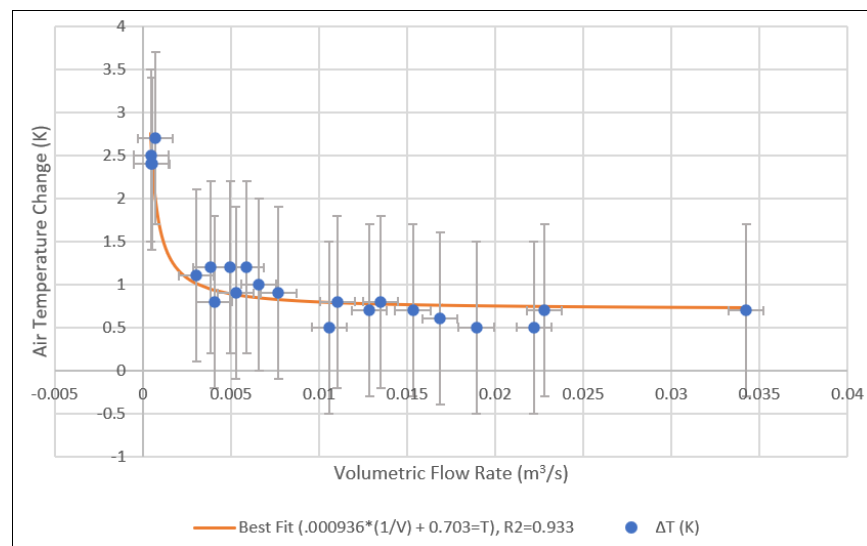


Figure 10: Graph Showing Temperature Difference (K) vs. Volumetric Flow Rate of Air

While the line of best fit generated has a relatively high R^2 ($=0.933$), which suggests a high correlation, the equation generated includes a large temperature shift ($=0.703$ K) that is not predicted by the specific heat capacity equation. There are many potential contributing factors to this observed difference. Primarily, as indicated by the size of the error bars on the data, the temperature readings on the thermocouples used were not accurate enough to ensure reliable data. For future experimentation, a more precise thermocouple should be employed. Furthermore, the flow rate may have varied within the pipe, as the speed of the air was only measured at the inlet of the pipe. Finally, the inversely proportional relationship between temperature and flow rate is true if the power input to the air flow is held constant, but, in reality, it is likely that there were variations in power input between experiments, as discussed below.

In order to understand the amount of heat being transferred from the panel to the air stream, the specific heat capacity equation was employed again to find the relationship between air flow rate and power output. For these calculations, the density of air was taken to be a constant at 1.225 kg/m^3 , and the specific heat of air was also taken to be a constant at 1.005 $\text{kJ}/\text{kg} \cdot \text{K}$. Figure 11 shows a graph of the anticipated power output of the system compared to the flow rate.

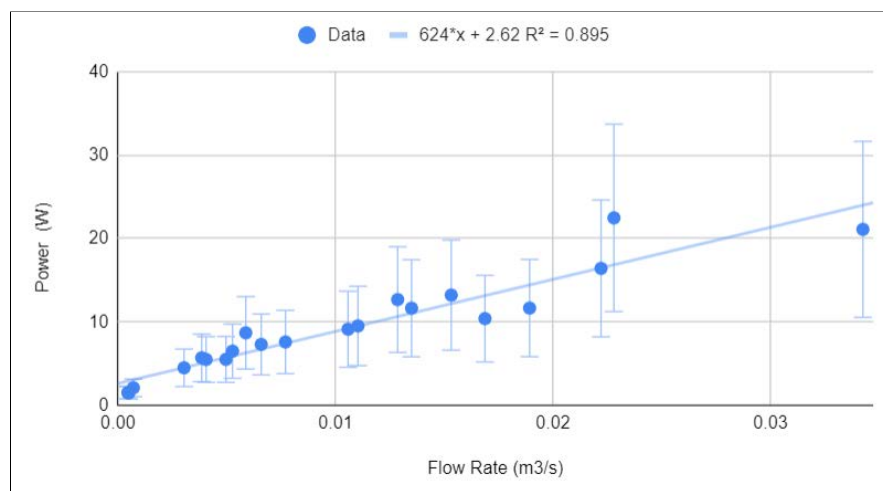


Figure 11: Anticipated Power Output (W) vs. Flow Rate (m^3/s)

As shown in Figure 11, a positive linear correlation was found between flow rate and power output. This trend is somewhat unexpected, as, given the same design set up, we would anticipate a consistent power output delivered by the heat pipes. Of course, the largest contributing factor to this relationship is likely the large amount of error associated with the measurements taken, so although there is a relatively high R^2 value ($=0.895$), there is low confidence in these results. Beyond the error associated in these measurements, there are a few potential physical contributing factors to this trend. The smallest flow rates are associated with a smaller pipe diameter (1.5 in); the smaller pipe diameter permits less of the heat pipe to be exposed to the air stream (as compared to the larger pipe of 3 in diameter) so there is a smaller surface area able to transmit heat into the air flow, which could result in less power being transferred into the air flow. Furthermore, it is possible that at higher flow rates, the air flow became more turbulent and warmed the air slightly more due to friction with the walls of the pipe. Given the low confidence in the power output, it was not possible for the team to conclude on an average power of the system; however, in order to proceed with environmental benefit analysis a power output of 10 W from the heat pipes to the airflow was assumed. In addition, it should be noted that the power outputs found are substantially lower than the output anticipated in the *Heat Transfer Theory and Calculations* section. Aside from errors in temperature measurement and the simplifications made in the calculations, this difference could also suggest that the heat pipes had less contact with the panel surface than anticipated, which could be improved upon in future designs.

While recognizing the limitations of these experiments given the uncertainties of the temperature measurements, the team recommends a larger diameter pipe for any practical applications; however for the final design a diameter of 1.5 in was used to obtain higher

temperature differences with less uncertainty. Additionally, while preliminary results suggest a positive correlation between volumetric flow rate and power output for our design, in an application where water is used to transfer heat away from the panel, a much slower flow rate would be utilized, both to yield a higher temperature increase and to be consistent with the application's plumbing requirements.

Panel Backing

Given the low temperature increase produced by the heat pipe configuration, the team hoped to increase the heat transferred from the surface of the panel to the heat pipes. The team tested two potential methods to increase heat transfer: 1. The team added a layer of insulation across the back of the panel and 2. The team added foil between the heat pipes and the panel and another layer of foil across the heat pipes. In both cases, the team observed a slight increase in the air temperature; however, in both cases the temperature of the panel was raised considerably (>5 °C), and thus both panel backing methods were abandoned to operate at lower panel temperatures.

Final Design



Figure 12: Final Prototype with 1.5" PVC Configuration

The final design consisted of a solar panel with six heat pipes inserted into the aluminum siding and into the same PVC tube from the component testing (shown in Figure 12). Thermocouples were set up at the inlet and outlet of the PVC air duct, on the surface of the panel, and underneath the panel. An anemometer was also used to find the air speed at the inlet to the tube (as well as the outlet for some trials, where there was a qualitatively noticeable difference in the air speed at each end). The bill of materials in Appendix B lists each component of the design and setup along with prices to yield a total system cost of \$134.41. This cost is the price of retrofitting the solar panel with the proposed system and is in addition to the cost of the panel itself.

CAD Simulations

The team modeled a solar panel in SolidWorks to simulate their lab based experiments and test their system under conditions more similar to their target of Hawaii that would be difficult to replicate in their lab setting. They added solar radiation at 1000 W/m^2 to their model, which is the standard used to test panels. They incorporated 22 heat pipes on the back of the panel that were designed based on the manufacturer's specifications and set the environmental temperature at 300 K. To match their lab testing, the team added a PVC pipe to the model. This pipe contained a fan that would cool one end of the pipes to remove heat from the panels.

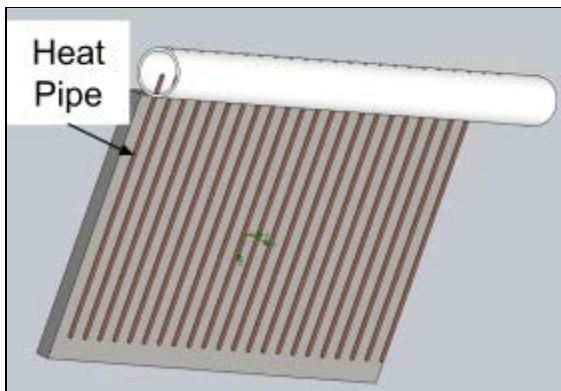
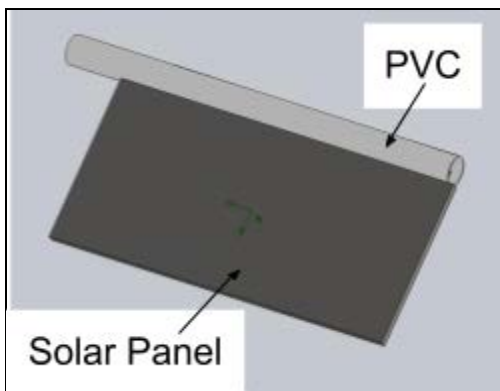


Fig. 13: Front View of Model System

Fig. 14: Back View of Model System

Initially, the team incorporated a 3" PVC pipe into the simulation to match the experimental setup.

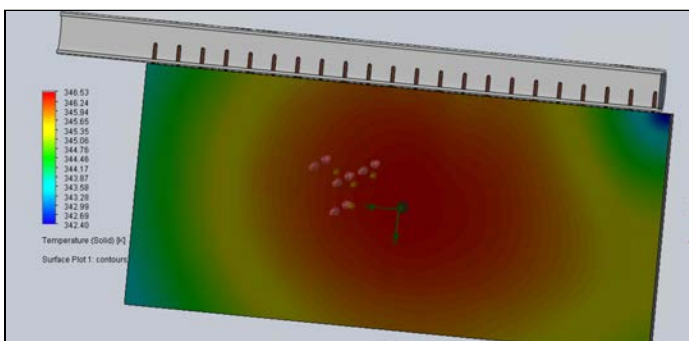
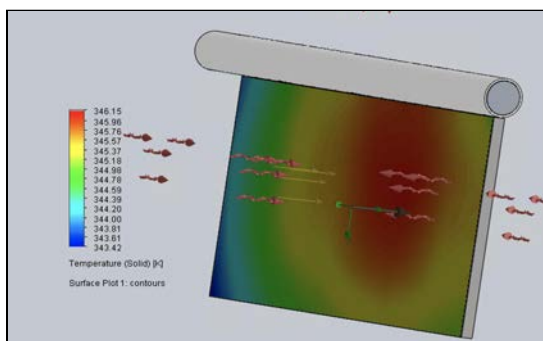


Fig. 15: 3" PVC and Natural Convection

Fig. 16: 3" PVC and Forced Convection

From Figs. 15 and 16, there is not a significant temperature difference between the system with forced convection compared to the system without.

Looking more closely at the PVC and impact of the fan:

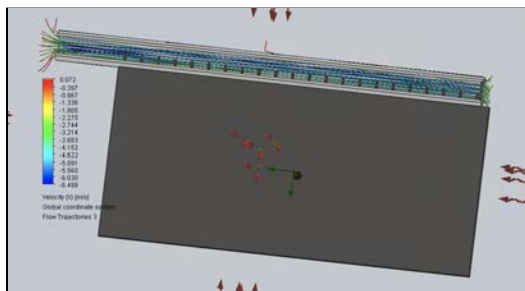


Fig. 17: Fan Velocity of 6 m/s

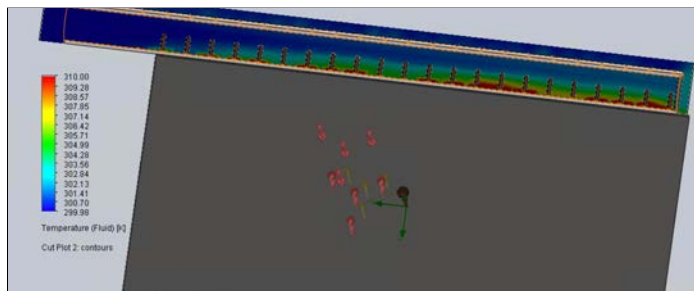


Fig. 18: Air Heated 1-3 °C

Figures 17 and 18 illustrate that the fan was removing air from the pipe at a rate of approximately 6 m/s, with a temperature increase of 1-3 °C at the pipe outlet. Thus, while the panel was not noticeably cooled, the system was able to deliver heated air.

The team repeated the simulations with a smaller PVC pipe with a 1.5” outer diameter, again to mimic laboratory testing.

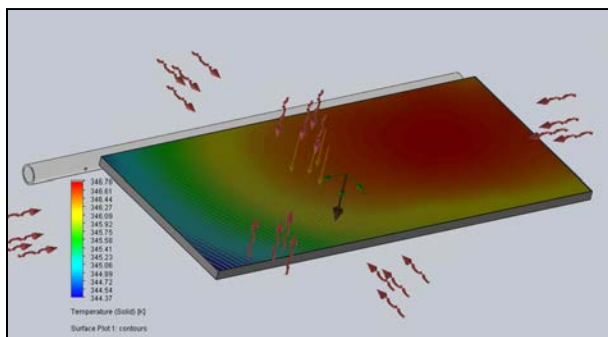


Fig. 19: System with Natural Convection

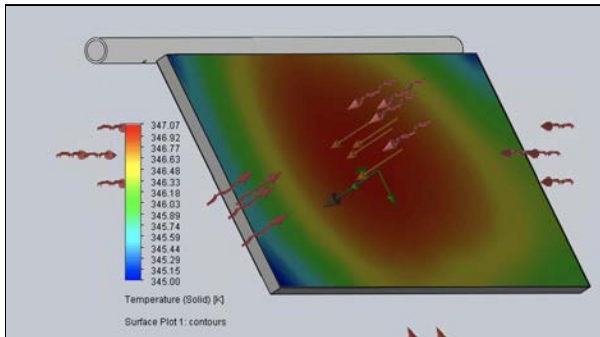


Fig. 20: System with Forced Convection

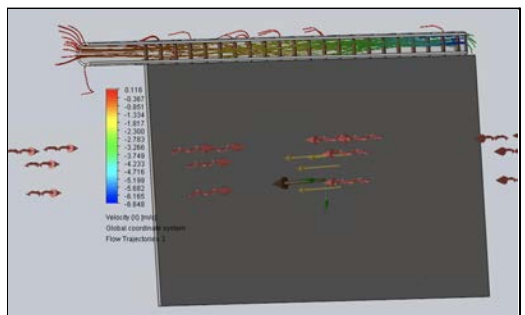


Fig. 21: Average Fan Velocity of 3 m/s

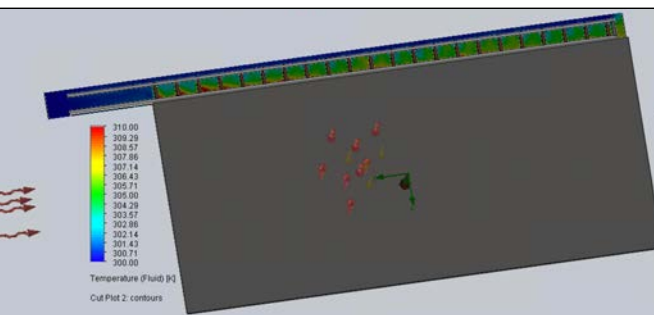


Fig. 22: Air Temperature Increase of 5 °C

Figures 19 and 20 illustrate that, similar to the system with the larger PVC pipe, there is less than a 1°C temperature difference between the simulation with forced and natural convection. The same fan was used for all simulations, but the air speed for this simulation was lower, with an average air speed of approximately 3 m/s. Additionally, this configuration yielded a higher temperature output, with the air heated by approximately 5 °C.

Initial simulations performed by the team were run at a mesh of four (meshes in SolidWorks Flow Simulation range from one to seven, with one being the least dense and seven being the most dense). The higher the mesh, the finer the minimum unit of analysis. These simulations yielded significant temperature decreases between the forced convection systems compared to the natural convection systems. The team increased their mesh to a five to yield more accurate results, and there was no longer a significant temperature difference. Future analysis could investigate the impact of increasing the mesh further and adjusting the mesh so that it is finer around the narrow heat pipes. This may reveal more significant temperature differences between the systems with forced and free convection.

Environmental Benefit Analysis

One of the primary environmental benefits of a solar-cell system is the generation of carbon-free energy. The quantity of energy produced will differ based on the size of the solar cell. However, for this system, the main environmental benefit is the additional energy collected in the form of heat due to the addition of heat pipes.

The thermal component of the PV-thermal system will also lead to energy savings and carbon savings, as the transferred heat can be supplied to a secondary use. For example, the team considered a use-case where the PV-T device could supply heat to a hot water storage tank. Water heating is an area where energy-efficiency could have a significant impact, as heating accounts for about 20% of a residential house's energy use (U.S. Department of Energy). Based on results from experimentation, the team estimates that the current iteration of the design delivers 10W of power. If this device can deliver 10W for five hours of the day, for $\frac{3}{4}$ of days throughout the year, 13.7 kiloWatt-hours (kWh) of energy would be generated per solar panel per year. If 13.7 kWh were supplied by natural gas instead, 2.8 kilograms of carbon dioxide would be emitted. The quantity of carbon dioxide emitted was calculated by assuming that the methane was burned in a combustion reaction. The work can be seen in the appendix. Additionally, further improvements in the thermal system would lead to further reductions in carbon emissions.

The excess heat captured from the solar panel could also be used to heat air in municipal buildings. This will reduce the need to heat space with traditional natural gas systems. A similar analysis as performed above could be conducted to demonstrate the carbon savings.

An additional source of environmental impact is the mining and manufacturing of the materials that the design requires. This report proposes the addition of PVC and copper heat

pipes to traditional solar panels. Traditional solar photovoltaic systems have their own environmental impacts, with Life-Cycle Assessments finding that there are significant outputs of solid waste and water pollution (Mahmud et al., 2018). There have been past studies on the feasibility of panel recycling. Unfortunately, studies have concluded that panel recycling efforts are extremely underdeveloped and that more work is needed to make recycling safe and implementable (Xu et al., 2018).

Further, copper must be mined to make the heat pipes. The impacts of this include energy use (average of 22.2 GJ/t Cu) to remove the copper, consumption of water in the mining processes (average of 70.4 kL/t Cu), and associated greenhouse gas emissions (average of 2.6 t CO₂-e/t Cu) (Northey et al., 2013). It is possible to recycle copper, and most new copper scrap is diverted from landfills and recycled (Gómez et al., 2007). This can help improve the sustainability of the design proposed in this report.

Moreover, PVC has a negative impact on the environment. Compared to Polypropylene and Polyethylene, it is the most energy intensive to produce and results in the most greenhouse gas emissions. CO₂ is released in the production of PVC. Solutions do exist to reduce the impact of PVC, including the development of new PVC using recycled PVC and the collection of CO₂ emissions at manufacturing facilities, where membranes are added to capture CO₂ (Alsabri & Al-Ghamdi, 2020).

Target Market and Basic Business Plan

The combined photovoltaic-thermal system, in its current design, is not marketable for a wide range of applications. The primary implementation of this PV system would be assisting a heat-pump system used to heat and cool a building. However, there are several obstacles to integration and effectiveness of this heat-pump enhancement. First, the peak output of the PV-T system may not align with the customer's needs from the heat pump. The heat pipes generate hot air, especially during periods of prolonged sun exposure and high levels of ambient temperature, typically found during the summer months. However, the customer during these summer months will not be heating their home or office - rather, the building will be reversing the flow of the heat pump so hot air flows out of the building. Therefore, the heat pump would not be able to take advantage of the PV-T system except during colder months when the customer is utilizing hot air. With colder temperatures and lower levels of insolation, the PV-T system is least efficient when the heat pump has the highest need for its product. This application for our product is impractical and further research is necessary if this current design is brought to market.

The market for our PV-T design is much broader if the current working fluid (hot air) is replaced with water. Hot water is needed year round for a myriad of applications, including residential and industrial water systems. Our industrial market plan focuses on expansion of PV-T into federal buildings, especially those being renovated or constructed. Newly constructed federal buildings, along with those undergoing significant renovations, must provide at least 30% of their hot water from solar hot water collectors (NREL, 2015). This requirement aligns with our product's ability to produce hot water and a large-scale agreement with the federal government decreases the cost of implementation. Our primary residential market would be large, multi-home complexes with central water heating systems. Examples of locations are

hostels, dormitories and multi-story apartment complexes. Potential customers would be the owners of these complexes, rather than individual renters, and the federal government.

Additionally, our PV-T system is most effective in areas with high levels of insolation, high ambient temperatures throughout the year, high water costs or limited water supplies, and high cost of electricity. Thus, the biggest market in the United States would be the American Southwest, including California and Texas. Other, smaller domestic markets would be Hawaii, Puerto Rico, American Samoa, and Guam, along with other military bases throughout the South Pacific. Internationally, the PV-T system is most effective in tropical and subtropical latitudes including Southeast Asia and the Mediterranean region, such as Italy, Greece, and North Africa.

The basis of our industrial market plan is a National Renewable Energy Laboratory (NREL) simulation of PV-T implementation across the country at federal building sites. The experiments simulated PV-T systems in six different US cities in a variety of climate zones operating with different utility scales. The simulation included 144 solar panels accompanied by solar installer collectors separated into three hot water loops. Each loop fed into two 80-gallon tanks for a total storage capacity of 480 gallons. The payback findings of the study are found below in **Table 2** (NREL, 2015).

Table 2: NREL Simple Payback Comparison between U.S. Cities

City	Electricity Rate (\$/kWh)	City Cost Adjustment Multiplier	Solar Energy Production (kWh/yr)	Annual Cost Savings (\$)	Installed Cost (\$)	Simple Payback (yrs)
Portland, OR	0.0868	0.992	6,698	\$581	\$56,765	98
Boston, MA	0.1476	1.172	6,331	\$934	\$67,065	72
Denver, CO	0.1083	0.943	11,063	\$1,198	\$53,961	45
Honolulu, HI	0.3454	1.173	10,097	\$3,488	\$67,123	19
Daggett, CA	0.1813	0.996	11,824	\$2,144	\$56,994	27
Phoenix, AZ	0.105	0.887	11,783	\$1,237	\$50,757	41

Of the six cities, only Honolulu, HI and Daggett, CA met federal requirements for life-cycle costing. To achieve this requirement, the system must have a simple payback period of less than 40 years. However, all cities except Portland, OR were able to meet these life-cycle costing requirements with the addition of a 30% federal subsidy. A deeper analysis of the cost per solar panel is found in **Table 3** (NREL, 2015).

Table 3: NREL System Components and Cost

Installed Costs		
PV-T System Components & Labor	Price	Dealer Price
SDK400 kit	\$43,200	\$32,400
Collector Installation Labor	\$1,440	\$1,080
Solar Storage Tank/w heat exchanger	\$4,800	\$3,600
External H/E (Pool)	\$400	\$300
Plumber (Tank Connections)	\$2,100	\$1,575
Plumber (HE Connections)	\$1,400	\$1,050
PEX + cladding	\$400	\$300
PEX Installation labor	\$400	\$300
Contingency (2%)	\$3,083	\$2,312
Total PV-T Components & Labor	\$57,223	\$42,917

The majority of the costs stem from the solar cell, the solar water collector, and the plumbing system. Our heat pipe implementation allows for this cost to be reduced, or at least offset, by the additional heat provided from the PV-T system. As solar panels become cheaper, this PV-T approach is more viable in the coming years.

Although our experiments did not reveal any increase in efficiency of the solar cell, an optimal scenario includes more efficient solar cells as heat is drawn away from the panel. An experimental, residential PV-T system saw a 2% increase in electrical efficiency and saw a 34°C panel temperature decrease, when compared to a PV panel that was not actively cooled (Sevela & Olesen, 2013). A review of PV-T analyses revealed that the efficiency improvements were consistently negligible, with only one of the six studies analyzed reporting an increase in

efficiency. **Table 4** below compares the thermal and electrical efficiency reports from each of the six studies (Farshchimonfared et al, 2016). Further research is needed before an increase in electrical efficiency can be quantified as a marketable asset of our PV-T System.

Table 4: Comparison of Efficiencies of Previous Studies (Farshchimonfared et al, 2016)

Results of previous studies of PV/T air collector(s) and their associated air distribution system.

Author(s)	\dot{Q}_f / η_{th}	\dot{W}_{pv} / η_{el}	\dot{W}_{fan}	$\dot{Q}_{eff} / \eta_{Overall}$
Hegazy (2000)	25% increase in thermal efficiency	1.2% increase in electrical efficiency	Increased from 0.03 kW h/day to 10 kW h/day	Significant efficiency drop when $\dot{m}/A_c > 0.03$ or $\dot{m}/A_c < 0.02$ kg/s m ²
Tiwari et al. (2006)	Not reported	Not reported	Not reported	Significant efficiency drop when $V_{avg} > 2$ m/s ($\dot{m}/A_c > 0.06$ kg/s m ²) Overall efficiency increased by an increase in \dot{m}/A_c
Tiwari and Sodha (2007)	Not reported	Electrical efficiency remains constant at 10%	Not reported	Overall efficiency increased by an increase in \dot{m}/A_c
Tonui and Tripanagnostopoulos (2007)	25% increase in thermal efficiency	Around 1% increase	Significant increase in fan power (around 50%)	Not reported
Sarhaddi et al.(2010)	The maximum thermal exergy efficiency was 2% for an air velocity of 4.5 m/s	Electrical efficiency remains constant at 10%	Not reported	The maximum overall exergy efficiency is 11.1% at the air velocity of 4.5 m/s ($\dot{m}/A_c = 0.225$ kg/s m ²)
Bambook (2011)	Around 14% increase in thermal efficiency	Approximately constant electrical efficiency	Significant increase in fan power	Significant decrease in efficiency when $\dot{m}/A_c > 0.05$ kg/s m ² or $\dot{m}/A_c < 0.03$ kg/s m ²
Sohel et al. (2014)	Around 50% increase in thermal efficiency	Approximately constant electrical efficiency	Not reported	Significant increase based on energy balance method (40%)/slight increase based on exergy method

However, there could be scenarios in which even this marginal increase in efficiency could be useful. In places where electricity is quite expensive, there is consistently high amounts of insolation, and limited space for both solar water heaters and solar panels, this product would be quite useful. Perhaps island nations and developing countries in the tropics, such as the Philippines or Indonesia, would find several practical applications for this PV-T system. Using a multi-panel setup on a large multi-family residential complex could increase the efficiency of the system and decrease the payback period of the overall PV-T setup, when compared to using a single solar panel.

Other Considerations

There are several other next steps that could be taken to make further progress towards implementation and analysis of a full scale heat pipe-based PV-T system. The team's final deliverable involved only one solar panel, but in practical implementation, the full system would include heat harvesting from whole arrays of solar panels. With more solar panels to expand the PV-T system to, there would be additional costs from the increased number of heat pipes, fixtures, and piping. However, it may be possible to achieve higher temperature differences of the working fluid which would yield increased benefits in the form of hotter air or water. It may be valuable to investigate other types of piping or insulation that can be used to minimize heat loss from the working fluid through the piping to the surroundings.

Another consideration for scaling up the system would include logistics and cost of installation, monitoring, control, and maintenance of the PV-T system. Monitoring and control of the system would involve placing sensors to continuously measure and log temperatures of the panels, temperature of the working fluid at the inlet and outlet of the system, and the flow rate of the working fluid. Monitoring of these system parameters would be important in order to adjust flow rates as needed and detect any anomalies or system failures. Installation and maintenance of the system would be streamlined by making the system as modular and standardized as possible. This could involve making standard arrays of heat pipe configurations and piping that can be quickly retrofitted to existing solar panels.

Thorough additional testing and experimentation to analyze and optimize these other considerations should be done in order to minimize costs and challenges in future scaling and implementation processes.

Conclusion

This paper outlines the development process and experimental results of a PV-T system utilizing heat pipes. Heat pipes were chosen as the main heat transfer mechanism for this investigation because of their high thermal conductivities and prevalent uses in similar electronics heat transfer applications. Several preliminary experiments were run prior as a part of the development process of a full system prototype. These experiments included observing the power output of available solar panels, conduction in the heat pipes from heated metal plates to still air, and conduction in the heat pipes from heated metal plates to moving air. These experiments generally helped support the existing theory of heat pipe operation but did not produce strong enough results to confirm the trends provided by the literature and manufacturer. Next, the panel was combined with an array of six heat pipes and a forced convection system with anticipation of raising the air's temperature via extracted waste heat from the panel. Observed temperature differences rarely exceeded 2°C. Observed trends included output air temperature and air mass flow rate being inversely proportional and waste heat collected peaking at 25 W. However, this data cannot confirm these trends because of the limiting precision of the system's thermocouple measurements. The PV-T system in its current format is not marketable, limited both by inadequate performance and high cost. Specific markets with high insolation would need to be targeted and significant increases in heat transfer efficiency would need to occur for this technology to have market success. Suggestions to explore scaling and heat loss reduction were made for future projects.

References

1. Advanced Thermal Solutions. *Round Heat Pipe, part ATS-HP-D7L500S25W-144*. www.qats.com.
2. Ali, S., Hassanain, N. A. M., Ateeq, I. S., & Ghallab, F. (2021). *An Experimental Investigation on the Effectiveness of Integrated Heat Pipe-Water Immersion Cooling Technique on the Solar Panel's Performance* (SSRN Scholarly Paper No. 3994422). Social Science Research Network. <https://doi.org/10.2139/ssrn.3994422>
3. Alsabri, A., & Al-Ghamdi, S. G. (2020). Carbon footprint and embodied energy of PVC, PE, and PP piping: Perspective on environmental performance. *Energy Reports*, 6, 364–370. <https://doi.org/10.1016/j.egy.2020.11.173>
4. Anderson, W., Tamanna, S., & Sarraf, D. (n.d.). Heat Pipe Cooling of Concentrating Photovoltaic (CPV) Systems. *EMCORE, Inc.* Retrieved April 24, 2022, from <https://www.1-act.com/resources/tech-papers/heat-pipe-cooling-of-cpv-systems/>
5. *Convective Heat Transfer*. Engineering ToolBox. (n.d.). Retrieved April 24, 2022, from https://www.engineeringtoolbox.com/convective-heat-transfer-d_430.html
6. Dwivedi, P., Sudhakar, K., Soni, A., Solomin, E., & Kirpichnikova, I. (2020). Advanced cooling techniques of P.V. modules: A state of art. *Case Studies in Thermal Engineering*, 21, 100674. <https://doi.org/10.1016/j.csite.2020.100674>
7. Gómez, F., Guzmán, J. I., & Tilton, J. E. (2007). Copper recycling and scrap availability. *Resources Policy*, 32(4), 183–190. <https://doi.org/10.1016/j.resourpol.2007.08.002>
8. Habeeb, L., Ghanim, D., & Muslim, F. (2018). Cooling Photovoltaic Thermal Solar Panel by Using Heat Pipe at Baghdad Climate. *International Journal of Mechanical and Mechatronics Engineering*, 17(6), 6. https://www.researchgate.net/publication/329196967_Cooling_Photovoltai Thermal_Solar_Panel_by_Using_Heat_Pipe_at_Baghdad_Climate
9. Hammami, M., Torretti, S., Grimaccia, F., & Grandi, G. (2017). Thermal and performance analysis of a photovoltaic module with an Integrated Energy Storage System. *Applied Sciences*, 7(11), 1107. <https://doi.org/10.3390/app7111107>
10. *Home*. Advance Cooling Technologies. (n.d.). Retrieved April 24, 2022, from <https://www.1-act.com/resources/heat-pipe-resources/faq/>
11. International Energy Agency. (2021). *Net Zero by 2050*. <https://www.iea.org/reports/net-zero-by-2050>.
12. J. Dean, P. McNutt, L. Lisell, J. Burch, D. Jones, D. Heineke. *Photovoltaic-Thermal New Technology Demonstration - NREL*. January 2015. <https://www.nrel.gov/docs/fy15osti/63474.pdf>.
13. Madhuri, Pandey, A., Kumar, A., & Yadav, N. P. (2019). Predicting the performance of heat pipe at different inclination angle. *IOP Conference Series: Materials Science and Engineering*, 691(1), 012011. <https://doi.org/10.1088/1757-899x/691/1/012011>

14. Mahmud, M. A. P., Huda, N., Farjana, S. H., & Lang, C. (2018). Environmental Impacts of Solar-Photovoltaic and Solar-Thermal Systems with Life-Cycle Assessment. *Energies*, *11*(9), 2346. <https://doi.org/10.3390/en11092346>
15. M. Farshchimonfared, J.I. Bilbao, A.B. Sproul, Full optimisation and sensitivity analysis of a photovoltaic–thermal (PV/T) air system linked to a typical residential building, *Solar Energy*, Volume 136, 2016, Pages 15-22, ISSN 0038-092X, <https://doi.org/10.1016/j.solener.2016.06.048>.
16. Northey, S., Haque, N., & Mudd, G. (2013). Using sustainability reporting to assess the environmental footprint of copper mining. *Journal of Cleaner Production*, *40*, 118–128. <https://doi.org/10.1016/j.jclepro.2012.09.027>
17. P. Savela, B.W. Olesen. *Development and Benefits of Using PVT Compared to PV*. Department of Civil Engineering, Technical University of Denmark, 2013, https://oze.tzb-info.cz/download.py?file=docu/clanky/0120/012028_Development%20and%20benefits%20of%20using%20PVT%20compared%20to%20PV_clima2013.pdf.
18. Qpedia. (2009, August). *Advanced Thermal Solutions, Inc*. Retrieved from <https://www.qats.com/Qpedia-Thermal-eMagazine/Back-Issues-Content/62.aspx>.
19. Ross, Jr., R. G, and Smokler, M. I. *Flat-Plate Solar Array Project: Final report: Volume 6, Engineering sciences and reliability*. United States: N. p., 1986. Web.
20. Shockley, W., & Queisser, H. J. (1961). Detailed balance limit of efficiency of p-n junction solar cells. *Journal of Applied Physics*, *32*(3), 510–519. <https://doi.org/10.1063/1.1736034>
21. Skoplaki, E., & Palyvos, J. A. (2009). On the temperature dependence of Photovoltaic Module Electrical Performance: A review of efficiency/power correlations. *Solar Energy*, *83*(5), 614–624. <https://doi.org/10.1016/j.solener.2008.10.008>
22. Tonui, J. K., & Tripanagnostopoulos, Y. (2007). Improved PV/T solar collectors with heat extraction by forced or natural air circulation. *Renewable Energy*, *32*(4), 623–637. <https://doi.org/10.1016/j.renene.2006.03.006>
23. U.S. Department of Energy. *Water Heating*. <https://www.energy.gov/energysaver/water-heating>.
24. U.S. Energy Information Agency. (2022). *Solar power will account for nearly half of new U.S. electric generating capacity in 2022*. <https://www.eia.gov/todayinenergy/detail.php?id=50818>.
25. Xu, Y., Li, J., Tan, Q., Peters, A. L., & Yang, C. (2018). Global status of recycling waste solar panels: A review. *Waste Management*, *75*, 450–458. <https://doi.org/10.1016/j.wasman.2018.01.036>
26. Zhou, J., Zhong, W., Wu, D., Yuan, Y., Ji, W., & He, W. (2021). A Review on the Heat Pipe Photovoltaic/Thermal (PV/T) System. *Journal of Thermal Science*, *30*(5), 1469–1490. <https://doi.org/10.1007/s11630-021-1434-3>.

Appendices

Appendix A: Table of System Thermal Properties, Relevant Areas, and Relevant Lengths
(Engineering ToolBox. (n.d.))

Property	Value
Thermal conductivity, k, of the solar panel	150 W/(m*K)
Convective Heat Transfer Coefficient, h, of moving air in PVC pipe	~500 W/(m ² *K)
Thermal conductivity, k, of the heat pipe	100,000 W/(m*K)
Area of panel	0.55 m ²
Cross-sectional area of 1 heat pipe	3.84 x 10 ⁻⁵ m ²
Surface area of 1 heat pipe exposed to moving air in PVC	0.001 m ²
Thickness, L, of panel	0.05 m
Length, L, of heat pipe	0.5 m

Appendix B: Bill of Materials for Final Prototype

Item	Quantity	Price/Unit	Total Price
500 mm long, 7 mm diameter Round Copper Heat Pipe	6	\$15.11	\$90.66
San Ace 80 mm Fan	1	\$10.00	\$10.00
1.5" diameter, 3 ft long PVC Pipe	1	\$1.43/ft	\$4.29
Foam board insulation	1	\$10.00	\$10.00
3" to 1.5" PVC Reducer	1	\$6.46	\$6.46
12V DC Power Supply	1	\$13.00	\$13.00
Total			\$134.41

Appendix C: Thermal Resistor Network Model

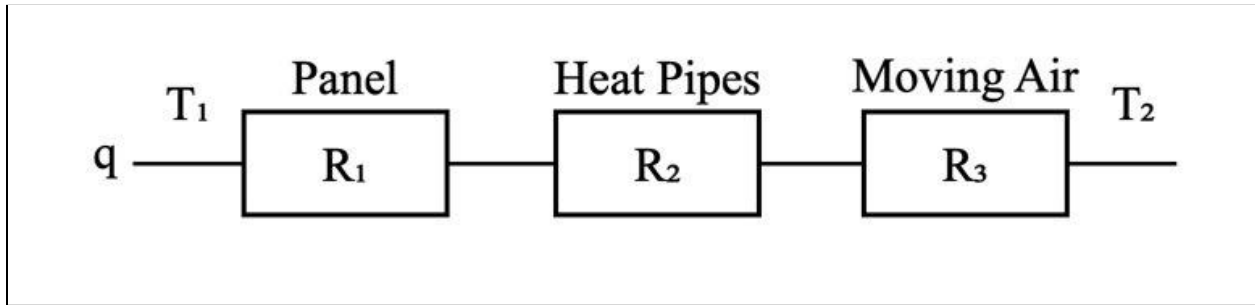


Figure 22: Visual depiction of the mathematical model used to predict waste heat capture

Appendix D: Carbon Emission Calculations

Carbon Emission Analysis

System provides 10L.

$$10L \cdot 5 \text{ hr/day} \cdot \frac{3}{4} \cdot 365 \text{ days} = 13.7 \text{ kWh}$$

$$13.7 \text{ kWh} = 49,320 \text{ kJ generated per year}$$

specific heat of natural gas = 48.7 MJ/kg
 Assume natural gas = CH_4

Combustion Reaction (Note: $\text{CH}_4 = 16.04 \text{ g}$, $\text{CO}_2 = 44.01 \text{ g}$)

$$\text{CH}_4 + 2\text{O}_2 \rightarrow 2\text{H}_2\text{O} + \text{CO}_2$$

$$49,320 \text{ kJ generated} \cdot \frac{1 \text{ kg CH}_4}{48700 \text{ kJ}} = 1.013 \text{ kg CH}_4 \text{ needed}$$

$$1.013 \text{ kg CH}_4 \cdot \frac{1000 \text{ g}}{1 \text{ kg}} \cdot \frac{1 \text{ mol CH}_4}{16.04 \text{ g CH}_4} \cdot \frac{1 \text{ mol CO}_2}{1 \text{ mol CH}_4} \cdot \frac{44.01 \text{ g CO}_2}{1 \text{ mol CO}_2}$$

$$= 2,779 \text{ g CO}_2 = \boxed{2.8 \text{ kg CO}_2 \text{ emitted}}$$

Figure 23: Calculations analyzing carbon emissions for natural gas heating system